Photoproduction of Charged Pion Pairs from Hydrogen with Gamma Energies up to 1500 MeV*

LYMAN J. FRETWELL, JR.,† AND JOE H. MULLINS
California Institute of Technology, Pasadena, California
(Received 26 October 1966)

Charged-pion-pair photoproduction has been investigated up to a γ energy of 1500 MeV, using the Caltech 12-in. heavy-liquid bubble chamber with a small-diameter, high-intensity photon beam passing through a central beam-tube gaseous hydrogen target surrounded by the sensitive Freon. Scanning, analysis, and data-reduction techniques have been developed to deal with the problems of two-view stereo, hidden-event origins, absence of magnetic field, and the range-energy and multiple-scattering relationships that occur in the heavy materials. Roughly 5700 pictures have been scanned and analyzed, yielding 754 acceptable events. Cross-section and parameter distributions are generally consistent with the results of previous experiments. The total cross section rises sharply from near zero at 500 MeV to order 80 μb at 650 MeV, then falls slowly to 40 μb at 1500 MeV. The presence of the ρ^0 is clearly seen in the pion pair production at higher energies.

I. INTRODUCTION

CONSIDERABLE effort has been expended in the past few years on the photoproduction of charged pion pairs.[1–16] This report contains the result of analysis of 754 pion pair events using the Caltech heavy-liquid bubble chamber with a central hydrogen target tube, and a synchrotron endpoint energy of 1532 MeV. This event sample came from approximately 5700 of 52 000 pictures taken in one month; there are no plans at present to analyze the remainder of the film.

Film was multiply scanned in general since scanning efficiencies were low. Event candidates were analyzed on a measuring table connected to an overhead projection scanner. Computer processing consisted of track reconstruction with subsequent fit to all reasonable pion-pair photoproduction hypotheses; no competing hypotheses (e.g., three-pion production) were investigated. Final results are the total pion pair photoproduction cross section as a function of gamma energy and a limited investigation of possible contributing models. Chamber efficiency and model contributions were evaluated by means of a Monte Carlo event-generation computer program. Angular distributions were investigated but are not presented here since they appear to be consistent with those previously reported,[9,14–16] and the effects of chamber efficiency are difficult to unfold from the data.

II. EXPERIMENTAL ARRANGEMENT

Figure 1 shows a schematic view of the bubble chamber. Dark-field illumination for the stereo camera is provided by a Lucite-lens light-focusing system above the chamber. The pulsed-resonant expansion system is described elsewhere.[17] The target beam tube containing hydrogen at 50-atm pressure passes along a diameter of the chamber. It is made of stainless steel ranging in thickness from 0.03 in. at the narrow end to 0.08 in. at the broad end, coated with Kel-F on the outside to eliminate boiling. The 4.5° conic-section half-angle was chosen to reduce shower development in the visible region of the chamber, but in fact it could have been decreased somewhat as the design was overly conservative. The heavy liquid used was Freon (CF_3Br), with a density of 1.5 g/cm^3 and a radiation length of 11.5 cm. There was no magnetic field on the chamber; particle momentum measurement was obtained from the range-energy relationship for stopping particles (65% of our events had at least one stopping particle), and from a very crude measurement of track multiple scattering.

The experimental area is pictured in Fig. 2. The softest component of the photon beam ($E_\gamma < 20$ MeV) was preferentially removed by passing the beam through a beam hardener consisting of 74 g/cm^2 of LiH in a pulsed magnetic field. The double-collimation scheme shown

* Work supported in part by the U. S. Atomic Energy Commission. Prepared under Contract No. AT(11-1)-68 for the San Francisco Operations Office, U. S. Atomic Energy Commission.
† Present address: Bell Laboratories, Whippany, New Jersey.
[1] V. A. Peterson and I. G. Henry, Phys. Rev. **96**, 850 (1954).
[2] M. Sands, M. Bloch, J. G. Teasdale, and R. L. Walker, Phys. Rev. **99**, 652 (1955).
[3] V. Z. Peterson, Bull. Am. Phys. Soc. **1**, 173 (1956).
[4] R. M. Friedman and K. M. Crowe, Phys. Rev. **105**, 1369 (1957).
[5] M. Bloch and M. Sands, Phys. Rev. **108**, 1101 (1957).
[6] M. Bloch and M. Sands, Phys. Rev. **113**, 305 (1959).
[7] D. D. Elliott, Ph.D. thesis, California Institute of Technology, 1959 (unpublished).
[8] J. M. Sellen, G. Cocconi, V. T. Cocconi, and E. L. Hart, Phys. Rev. **113**, 1323 (1959).
[9] B. M. Chasan, G. Cocconi, V. T. Cocconi, R. M. Schectman, and D. H. White, Phys. Rev. **119**, 811 (1960).
[10] J. R. Kilner, R. E. Diebold, and R. L. Walker, Phys. Rev. Letters **5**, 518 (1960).
[11] D. McLeod, S. Reichert, and A. Silverman, Phys. Rev. Letters **7**, 383 (1961).
[12] R. Del Fabbro, M. de Pretis, R. Jones, G. Marini, A. Odian, G. Stoppini, and L. Tau, Phys. Rev. Letters **12**, 674 (1964).
[13] R. Del Fabbro, M. de Pretis, R. Jones, G. Martini, A. Odian, G. Stoppini, and L. Tau, Phys. Rev. **139**, B701 (1965).
[14] H. R. Crouch, Jr., *et al.*, Phys. Rev. Letters **13**, 636 (1964); **13**, 640 (1964).
[15] H. R. Crouch, Jr., *et al.*, in *Proceedings of the International Symposium on Electron and Photon Interaction at High Energies*, edited by G. Höhler *et al.* (Deutsche Physikalische Gesellschaft, Hamburg, 1965).
[16] U. Brall *et al.*, DESY Report No. 65/11, 1965 (unpublished).
[17] J. H. Mullins, E. D. Alyea, Jr., and J. M. Teem, in *Proceedings of an International Conference on Instrumentation for High-Energy Physics* (Interscience Publishers, Inc., New York, 1960).

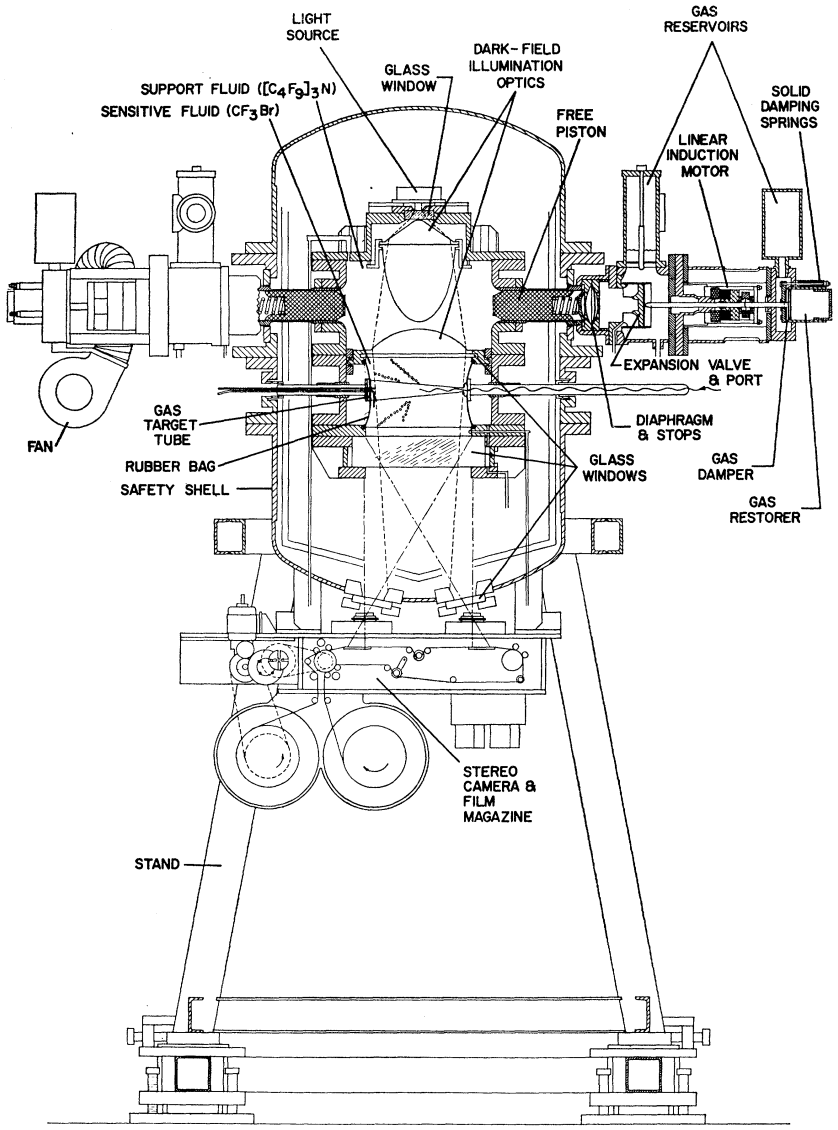

FIG. 1. The Caltech heavy-liquid bubble chamber.

rendered the small-diameter beam more circular as well as removing photons and electrons produced in the LiH. The combination of sweeping and post-collimation eliminates the enhancement of lower-energy γ rays which would otherwise occur through electromagnetic cascade processes in LiH. Beam size was kept small at the chamber ($\frac{1}{16}$-in. diam) since adequate synchrotron intensity was available for the average intensity of 3.1×10^5 equivalent quanta per pulse used in this experiment. A vacuum-beam tube, sweeping field, and lead scraper were used between the second collimator and the 0.008-in. Mylar window to the central beam tube target.

The usual Cornell-type ion chamber was not used to monitor beam intensity for two reasons. One was the possibility of saturation effects during the fast beam dump required by the bubble chamber, which, however, turned out to be negligible because of the small beam intensity. The other was the existence of considerable premature beam spill, to which the ion chamber was sensitive and the bubble chamber was not. This averaged 5 to 10% of the total intensity at this energy. Beam intensity was recorded by integrating the gated output of counter a telescope looking at a polyethylene target in the beam downstream of the bubble chamber. Since the chamber could cycle no faster than once every three synchrotron pulses, the other two pulses were taken using slow spill; the telescope output was integrated on another scaler and the beam intensity was monitored by integrating the output of an ion chamber, thus providing continuous calibration of the counter telescope during running. A lead pendulum called the "lead chopper" prevented the beam from reaching the ion chamber except during the calibration pulses. A scintil-

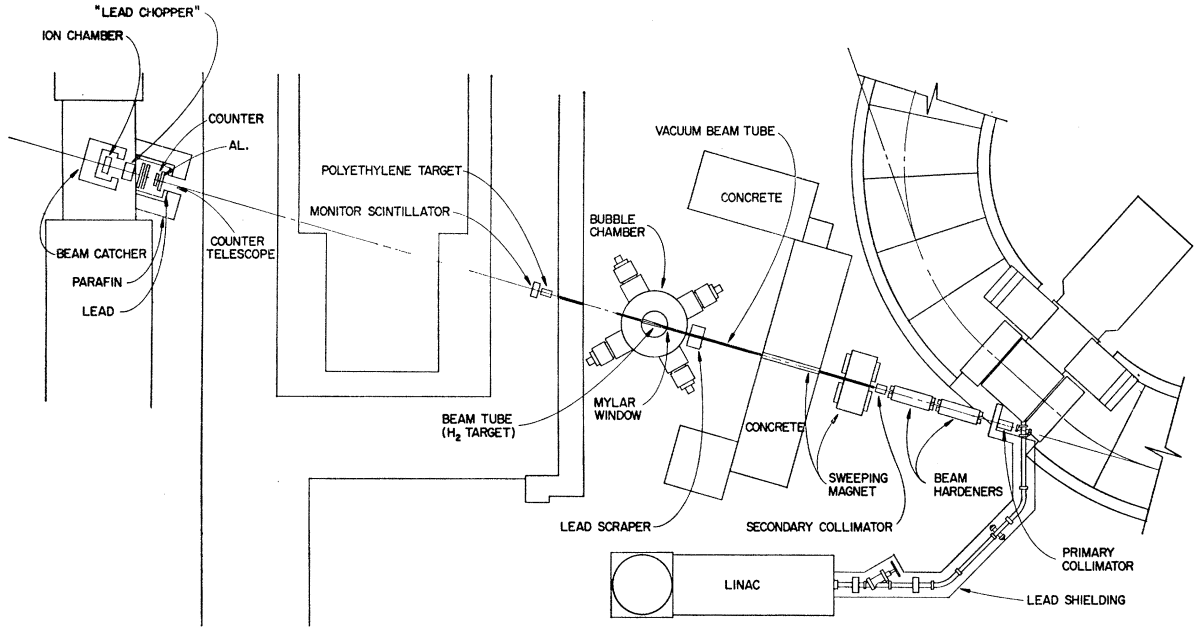

FIG. 2. The experimental arrangement and beam area.

lator mounted close to the polethylene target was used to monitor premature beam spill and beam timing during the run.

III. DATA ANALYSIS

Film scanning was directed toward finding all combinations of three or more tracks that appeared to come from the same location on the beam line. Because of the high beam intensity, tracks from different nuclear events could appear to have come from a common origin. The overhead projection scanner allowed alternate selection of the two stereo views, and controls permitted the two to be aligned with respect to each other so that the image of a real point on the beam line was in the same place on the scanning table in both views. The accuracy of mutual track lineup required for event acceptance varied with different track conditions. The person scanning could estimate the unseen path length through Freon and steel, and by looking at the multiple scattering in an equivalent length in the visible track region estimate how much the track might have scattered between the production origin and the point where it first became visible. The criteria by which a scanner would accept two tracks as belonging to a common event were much looser than those eventually applied by the computer analysis. For example, the distance between their apparent origins on the beam line acceptable to the scanner was approximately twice that acceptable to the computer. Occasional event rejection at the scanning table due to bad track scattering thus does not necessitate correction.

Despite extensive shielding around the bubble chamber, the large intensity of dumped beam caused numerous neutron- and gamma-induced tracks throughout the sensitive chamber volume. Such tracks were short, often only a single bubble in length, but they provided a background sea against which the desired proton and pion tracks had to be found. As a result, there were effectively minimal track lengths that could be found in scanning. For stopping particles this minimal chamber length, projected onto the plane of sight, was 0.5 cm. Average nonstopping proton and pion projected lengths were 1.5 and 2.0 cm, respectively. As might be expected, these nonstopping lengths were a function of bubble density (and hence particle velocity), and the explicit dependence of these lengths upon particle velocity, taken from the distribution for valid events, was included in the Monte Carlo event-generation procedure described below.

In addition to finding tracks, scanners recorded whether or not each track definitely stopped within the illuminated chamber volume (stopping tracks implied range-energy measurement). Multiple scattering and bubble density also permitted qualitative track identification. This identification was considered certain for stopping tracks with projected lengths >1.5 cm, and for nonstopping tracks with lengths >5 cm and particle momenta <250 MeV/c for pions and 750 MeV/c for protons, for reasons described later. Computer-event analysis tried all possible particle identifications for tracks; a subsequent survey of our valid events indicated that the qualitative particle identification had been better than 90% accurate, so that considerable confidence could be placed in particle identification even in the noncertain regions.

Event measurement consisted of fiducial point measurement and measurement of several points along each

track. The first measured point on each track was chosen to be the first point clearly seen, the second point was chosen to best indicate track direction, and subsequent points (usually one to four) were taken to reflect track length and multiple scattering. At each point an attempt was made to find bubble images in each view that corresponded to the same physical bubble in the chamber (called corresponding points), or if this was not possible, points were measured that would be close to the corresponding points. Events were remeasured as many times as necessary to rule out measurement error or to provide a clear pattern of success or failure. The average number of measurements per event candidate was 2.5.

Rather than try to adapt any of the extant data-reduction programs, we developed our own system of programs to deal with the problems of no magnetic field, track emanation from an unseen origin, multiple scattering, and the range-energy relationship in the liquid. Computer processing of events consisted of two principal phases: track reconstruction and event reconstruction.

Imaginary light rays from each film image point were traced back into the chamber and the mutually closest point to the light rays was calculated for each pair of pseudocorresponding points. If the two corresponding light rays passed within 0.01 cm of each other they were considered corresponding and the resulting closest point was taken to be the point on the track in the chamber. If not, an iterative procedure was used to arrive at the improved set of pseudocorresponding points. Effectively the film images from the above chamber point were located (they are necessarily corresponding, but in general do not lie on the track images). Then they were moved in such a way as to provide a simultaneous best fit to the original track segments in each view and the original points. During fitting, the two image points were moved so as to maintain their relative spacing, thus retaining approximate correspondence over small regions. Then these points were projected onto the original line segments, and those projected points were treated as pseudocorresponding points and iterated as described above. During program tests, it was shown that noncorresponding points chosen from computer-generated tracks converged toward corresponding points using this procedure. For data analysis, 20 such iterations were allowed, which usually proved sufficient except for tracks moving parallel to the line between the camera lenses, for which one must find real corresponding points.

IV. EVENT RECONSTRUCTION

The event-reconstruction program[18] employed a maximum-likelihood method to find the "best" event hypothesis. The program employed a modified version of a program called MIN[19] to find the most likely solution to the kinematic problem. The likelihood function included particle multiple scattering in the steel wall of the beam tube and the hidden regions of freon, measurement errors, and any information obtained from range or multiple-scattering measurements. All combinations of three prongs were attempted, with all possible combinations of particle identification. If all such combinations of an event failed the analysis, then the stopping restrictions, based on observed track lengths, were removed and the event reprocessed.

TABLE I. Scanning identification accuracy.

	Total percentage[a] incorrectly assigned	Percentage[a] with alternative not mentioned
Called proton, was pion	2.7	2.1
Called pion, was proton	10.8	7.1
Called stopping, was going out	0.2	0.1
Called going out, was stopping	1.5	1.3

[a] Percentages are based on the number of tracks of the appropriate type (proton, pion) among all the accepted events. For the stopping errors, the total number of tracks was used.

Several constraints were available to aid selection of the "best" event, and these were included in the likelihood functions. Besides the usual kinematic constraints, the events were required to originate on the rather small (~2-mm diam) beam line, as described earlier. In addition, rough multiple scattering measurements were made on each prong. These, however, were useful chiefly for obtaining starting values for the minimization procedure, without which convergence was sometimes impossible. In addition, approximately 65% of the events had at least one stopping particle, providing an additional kinematic constraint. An additional quasi-constraint was imposed by the visible track length for the nonstopping particles, i.e., the particle must have a minimum energy.

In cases where the computer program had changed a particle identification from that made by a scanner, had changed a "stopping particle" statement, or had found more than one acceptable hypothesis, the event was re-examined and often remeasured. The acceptance criterion was based on the χ^2, and in cases of doubt, on the credibility of the event seen on the scanning table.

It is interesting to note the accuracy with which the scanners were able to identify particles, as mentioned earlier. Table I shows the results, when the final, accepted events were compared to the scanner's original identification. It can be seen that particle identification averages about 90% accurate in the worst case. Closer examination of the data reveals that identification was about 95% accurate up to 250 MeV/c for pions and 750 MeV/c for protons when 5 cm or more of track was visible. Similar accuracy was attained for stopping particles with 1.5 cm or more of visible track.

[18] L. J. Fretwell, Ph.D. thesis, California Institute of Technology, 1967 (unpublished).

[19] W. C. Davidon, Argonne National Laboratory Report No. ANL-5990 Rev., 1959 (unpublished).

It was a great help in these identifications that the chamber sensitivity was extremely stable, and the bubble density was kept fairly low.

V. ANALYSIS EFFICIENCY

In order to test the efficiency of the program, a set of 99 events were generated by Monte Carlo techniques, including the effects of multiple scattering and measurement error. Of these, six were nearly coplanar events with no stopping prongs, and were thus not analyzed, which is the procedure followed with actual data. (Coplanar events of this type with no stopping particles are kinematically underdetermined.) The result of this test was that the program is $(96\pm2)\%$ efficient in correctly reconstructing real events.

Table II illustrates the behavior of the reconstruction program, as an example in which the "reconstructed" gamma energy is compared to the original value put into the generated event.

VI. ANALYSIS ACCURACY

Table III gives the average errors in the determination of the event parameters. These errors have been derived from the actual measured events, since one of the outputs of the minimization program is the expected error itself. The reliability of the error determination was checked against the Monte Carlo events. Coplanar production with no stopping particles is of course not included.

VII. SCANNING EFFICIENCY

One of the larger sources of error in the experiment, and the one most difficult to assess, is the scanning efficiency. Because of the very large track density in the photographs, special efforts were made to assess the scanning efficiency realistically.

Five regions of the film were set aside for scanning comparison regions, and all, with particular emphasis on one of them, were scanned very heavily and repeatedly, to attempt to find all event candidates. These regions were used to assess the scanning efficiency of the scanning personnel, as well as to check the analysis and scanning procedures. It was found, through checking the combined efficiency of several scanners, that the assumptions of an independent average scanning efficiency for each scanner was not tenable. This is merely a reflection of the fact that events varied greatly in their degree of difficulty, and it is easily shown that this situation leads to an apparent "correlation" in scanning efficiency.

TABLE II. γ-energy errors for analyzed generated events.[a]

	− − −	− −	−	0	+	+ +	+ + +
One or more stopping	0	2	16	13	18	8	0
No stopping tracks	1	4	13	3	12	2	1
Total	1	6	29	16	30	10	1

[a] Column code: 0: essential agreement with generated value. (+, −): (above, below) generated value, but within 1 standard deviation. (++, − −): (above, below) generated value, between 1 and 2.5 standard deviations. (+++, − − −): (above, below) generated value, outside 2.5 standard deviations.

TABLE III. Average parameter-measurement errors (in MeV) for valid events.

No. of stopping particles	γ energy range	γ energy	Dipion mass	Isobar mass
0		82.2	22.1	27.8
1		47.7	16.6	17.6
2		19.9	6.4	7.2
3		2.4	0.6	1.3
	Below 900 MeV	36.7	12.5	14.7
	900–1200 MeV	80.8	22.7	27.3
	Above 1200 MeV	93.9	28.0	27.0
Over-all average		54.3	16.7	19.2

At any rate, it was found that the following formula adequately (meaning within the errors assigned to scanning efficiency) describes the combinatorial properties of the scanning efficiencies:

$$E(x,y)=1-[(1-x)(1-y)+axy(1-x)(1-y)],$$

where

$E(x,y)=$ combined efficiencies of two scanners,

$x,y=$ scanning efficiencies of two scanners.

The equation may be viewed as strictly empirical. It was chosen to be symmetrical in the variables, to introduce a "correlation" term, and to return, approximately, the higher efficiency when a high efficiency was combined with a low one. However, a dependence of qualitatively this form can be expected from some reasonable physical assumptions.

Let the probability of finding the ith event by scanner No. 1 be denoted by ϵ_{1i}, and that by No. 2 by ϵ_{2i}. Then, from a total of N events, the number missed by No. 1 would be

$$M_1=\sum_i \eta_{1i}\equiv N\bar{\eta}_1,$$

where $\eta_{ji}=1-\epsilon_{ji}$, and $\bar{\eta}_j$ denotes an average over all events. Similarly, those missed by No. 2 are given by

$$M_2=\sum_i \eta_{2i}\equiv N\bar{\eta}_2.$$

Then the number missed by both would be

$$M_{12}=\sum_i \eta_{1i}\eta_{2i}\ [1-E(1,2)]N.$$

Now a simple expansion of the expression

$$\sum_i(\eta_{1i}-\bar{\eta}_1)(\eta_{2i}-\bar{\eta}_2)\equiv\sum_i(\Delta\eta_{1i})(\Delta\eta_{2i})$$

yields

$$\sum_i(\Delta\eta_{1i})(\Delta\eta_{2i})=-N\bar{\eta}_2\bar{\eta}_1+\sum_i\eta_{1i}\eta_{2i},$$

or

$$\sum_i\eta_{1i}\eta_{2i}=[(1-E(1,2)]N=N\bar{\eta}_1\bar{\eta}_2+\sum_i(\Delta\eta_{1i})(\Delta\eta_{2i}).$$

Therefore, observing that $\bar{\eta}_1=1-\bar{\epsilon}_1$, where $\bar{\epsilon}_1$ is the average efficiency of No. 1, we find

$$E(1,2)=1-\left[(1-\bar{\epsilon}_1)(1-\bar{\epsilon}_2)+\frac{1}{N}\sum_i \Delta\eta_{1i}\Delta\eta_{2i}\right].$$

If we assume that the efficiencies are positively correlated between scanners, that is, a difficult event is difficult for both scanners, then the second term in the brackets is always positive. Furthermore, if one scanner has uniformly high (near unity) efficiency, we expect the scatter ($\Delta\eta$) to be small. Likewise, if a scanner has uniformly low (η approaching unity) efficiency, we also expect the scatter to be small. In both cases the second term contributes little, and probably contributes most when the η's are around $\frac{1}{2}$. This is the general behavior of the empirical formula given above. This argument, of course, does not exclude such forms as $a[xy(1-x)(1-y)]^{1/2}$, which might be more reasonable on statistical grounds.

It was found that the scanning data were satisfactorily fit with the constant $a=1.5\pm0.5$. The constant was found to be a slight function of the section of film employed, but not (at least not strongly) of which scanners were involved. The formula was also found adequate for combinations of more than two scanners. The scanning multiplicity varied from one to seven scanners, consequently the final efficiencies also varied. The lowest scanning efficiency was $(77\pm8)\%$, the highest $(99.6\pm2.7)\%$. The average was between 85 and 90%, ± about 6%.

VIII. SCANNING BIAS

A difficult effect to evaluate was the degree of bias introduced by the varying scanning efficiency. The difficulty of finding events is a function of their nature, depending upon the particle types, energy, and length of visible track. As mentioned earlier, it is to be expected that a relatively slow particle would require considerably less visible projected track length to be easily seen than would a fast one, owing to the difference in bubble density. This effect, as well as the influence of the particle type, was studied by examining the distribution of track ends as a function of distance from the beam tube (projected track length). This yielded a minimum required visible length which was indeed a function of particle energy. This effect was quite important in evaluation of the chamber efficiency (below). Consequently, the error introduced by ignorance of the exact value of this function was evaluated by varying the track length cutoff over all reasonable values. The resulting uncertainty is included in the computed chamber efficiency. The average cutoff lengths used are given in Sec. III.

TABLE IV. Chamber detection efficiency.

γ energy (MeV)	Efficiency (%)	γ energy (MeV)	Efficiency (%)
450	5.8	1050	16.3
550	13.2	1150	14.5
650	14.4	1250	14.1
750	15.8	1350	14.1
850	16.2	1450	14.1
950	16.4		

IX. CHAMBER EFFICIENCY

The chamber efficiency was calculated from the results of an extensive Monte Carlo event-generation routine. Four models were selected for the production mechanism, and each was run to determine its detection efficiency, and the expected parameter distribution. These four were N_{33}^* isobar production, phase space, ρ° production, and σ-meson production (a $J=0$, $T=0$ π-π resonance at about 420 MeV).[12,13,20,21] 2500 visible events each of N^*, σ, and phase space were generated, and 500 of the ρ. For the resonant states, the probability distributions used were the phase space resonant enhancement ones of Jackson.[22] Resonance energy and width values employed were $N_{33}^*(1233,125)$, $\rho(740,115)$, $\sigma(420,100)$. Center-of-momentum angular distributions used were simple numerical approximations to the empirical distributions obtained by CEA[14,15] and DESY.[16] The manner in which these results were employed is discussed below. The chamber efficiencies used for calculation of total cross sections are given in Table IV.

X. BACKGROUND

The preponderance of competing processes (such as single-pion production) which can simulate a two-pion production made necessary a careful evaluation of the background. Possible sources of background are accidental spatial coincidences of two or more single- or multiple-pion production vertices, with some of the prongs lost in the beam tube or its shadow. Higher multiplicity of pion production can also simulate two-pion production if some of the prongs are lost. An occasional electron from pair, Compton, or knock-on production could also enter, although in most cases electrons are easily identified in the heavy liquid. To assess the background, sets of single, double, and triple pion production events were generated by the same Monte Carlo event-generation program used to assess the chamber efficiency. These generated events were based on the experimental cross section, and were combined (by using near coincident origins) when necessary to simulate a double pion event. (Relatively little of the background was contributed by pair and

[20] N. P. Samios, A. H. Bachman, R. M. Lea, T. E. Kalogeropoulos, and W. D. Shephard, Phys. Rev. Letters **9**, 139 (1962).
[21] Aachen, Birmingham, Bonn, Hamburg, London (I.C.), Munich Collaboration, Nuovo Cimento **31**, 485 (1964).
[22] J. D. Jackson, Nuovo Cimento **34**, 1644 (1964).

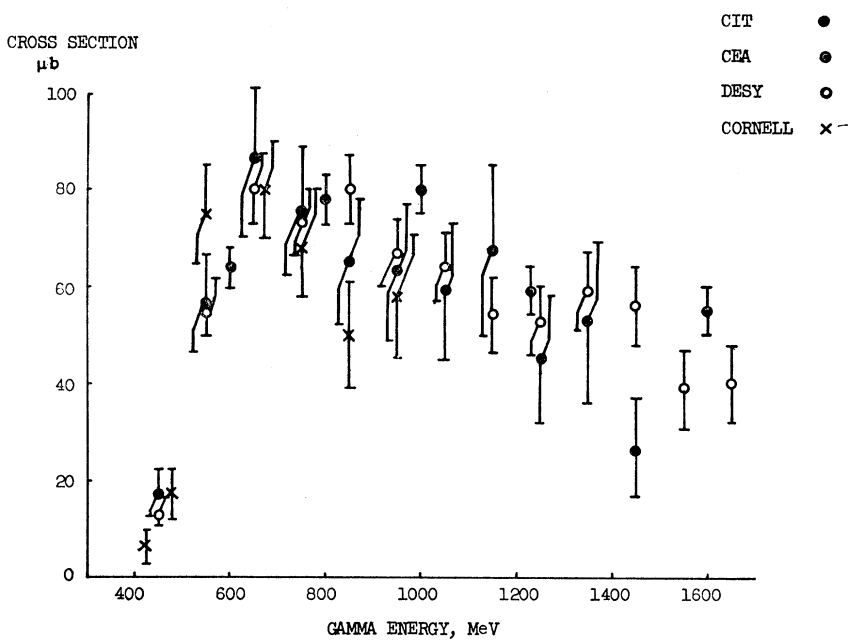

FIG. 3. Total cross section compared to that from other experiments.

higher-multiplicity pion production, so only approximate cross sections need to be known for these.) The results were then fed into the analysis program, and the acceptance rate determined. Knowing the yield of the processes, one can then calculate the frequency of coincidence. (Studies were also made of the spacing required of the origins to cause a "coincidence," i.e., to allow the event to be accepted.) Rate of production of false events due to γ conversion from π^0 decay was also studied.

The conclusion from the background study was that $(9\pm3)\%$ of the accepted events were background. The distributions of the background events with respect to γ-ray production energy, dipion invariant mass, and π-p invariant mass, were found to be quite similar to that for phase-space two-pion production. Consequently the background was subtracted from the phase-space contribution for the model fits, and subtracted as a simple 9% contribution, independent of γ energy, for the total-cross-section results.

XI. EXPERIMENTAL RESULTS

For purposes of deriving a total cross section, the events were divided into 100-MeV bins. The chamber efficiencies given in Table IV were used, having been calculated from the model fits of CEA and DESY. The numerical results are exhibited in Table V, and are plotted in Fig. 3, along with the data of CEA,[23] DESY,[16] and Cornell.[9] It should be emphasized that the errors indicated include *all known sources*, both statistical and systematic. Probable errors in scanning and analysis efficiency, in chamber efficiency, including uncertainty in the model fits, and in beam monitoring, among others, are included in the quoted errors. The rather good agreement with the other data would seem to indicate that the errors have been somewhat overestimated, but as we consider this more of a virtue than a vice, no reassessment has been made.

In addition, some attempts were made to see how the data agreed with previous CEA and DESY work with respect to the contributing models. It must be borne in mind that the separation of N_{33}^* and phase space is not expected to be as reliable in this work as in that of DESY and CEA. The reason is primarily that it was not possible to tell the π^+ from the π^- in this experiment as it is in a hydrogen chamber with magnetic field. The two distributions, in the absence of this identification, are very similar indeed, and their relative contributions are very sensitive to choice of the resonance energy. This is particularly true in the low γ-ray energy region. Nevertheless, the fits, as they emerged from the computer, are displayed below.

TABLE V. Yield and total cross section for this experiment.

Gamma energy (MeV)	Yield (events)	Total cross section (μb)
450	18	17.2± 5.1
550	105	56.5± 9.9
650	142	86.6±14.9
750	114	75.5±13.9
850	87	65.0±13.0
950	75	63.0±13.7
1050	63	59.3±14.0
1150	58	67.3±17.1
1250	35	45.2±13.2
1350	38	52.0±16.1
1450	17	26.2±9.7

[23] U. Maor (private communication).

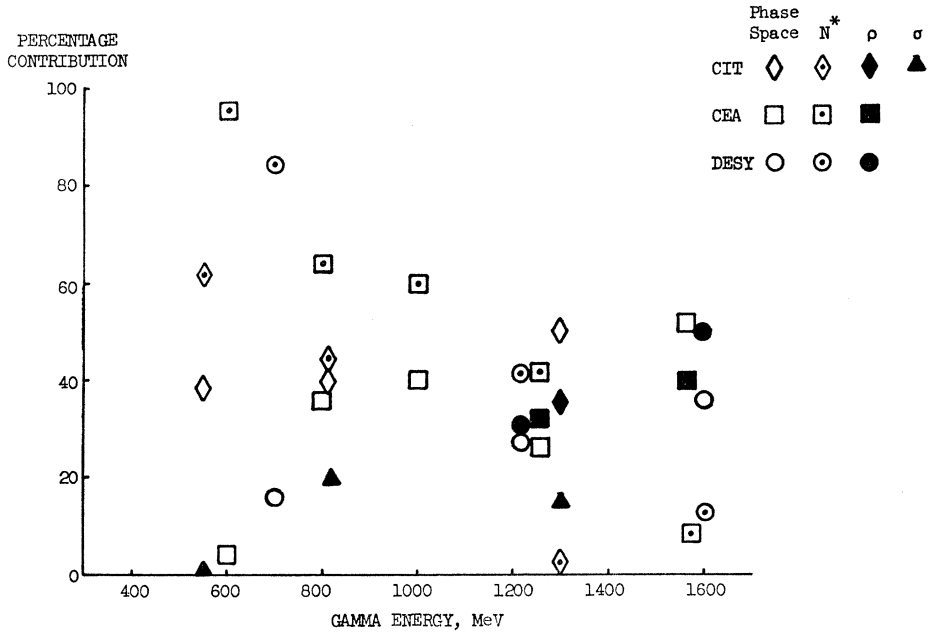

FIG. 4. Model fits compared to that from other experiments.

The events were broken into 40-MeV diparticle mass bins and compared to the computed Monte-Carlo distributions in γ-ray energy, dipion mass, and π-p mass, resulting from the various models. The contributions of the different models were then adjusted by means of the variable metric minimization program until a best fit was attained to the data, in all three parameters. No allowance was made for interference effects, and the 9% background was simply subtracted from the phase space contribution. The fit was made over three energy intervals: $E_\gamma<600$, $600<E_\gamma<1060$, and $E_\gamma>1060$. Two fitting attempts were made, one employing only the N_{33}* and phase space, the other all four models. The results are shown in Table VI. The errors quoted include the errors in the data and the statistical errors in the Monte Carlo–generated events.

TABLE VI. Parameters from model fit to data.

	Percentage contribution		
	$E_\gamma<600$ MeV	$600<E_\gamma<1060$ MeV	$E_\gamma>1060$ MeV
	Four-model fit		
Phase space	48.0±19.6	40.0±11.4	63.1±16.1
N_{33}*	61.1±22.5	40.5±9.3	−12.6±12.9
σ	−9.1±13.0	19.5±7.8	14.1±7.9
ρ	...	...	35.4±7.3
Fit χ^2	12.4	15.8	37.5
Degrees of freedom	8	21	31
χ^2 probability	13%	77%	19%
	Two-model fit		
Phase space	47.1±19.3	56.5±9.6	110.4±13.1
N_{33}*	52.9±19.3	43.5±9.6	−10.4±13.1
Fit χ^2	13.5	20.6	59.1
Degrees of freedom	8	21	31
χ^2 probability	10%	49%	0.1%

It can be seen that either set gives an adequate fit, though rather poor in the low-energy region, except that the two-model fit fails badly in the high-energy region. This is doubtlessly owing to the presence of ρ°, which is also visible as a distinct bump in the dipion spectrum of the raw data. The ρ° is clearly necessary to provide a good fit. Nothing definite can be said concerning the existence of the σ, even though a somewhat better fit is attained using it in the medium-energy region, and the raw data show a small bump at this dipion energy.

Figure 4 compares this model fit to that of CEA and DESY. Only the four-parameter fit is exhibited. There is a significant disagreement with the CEA and DESY values in the lower-energy region, for the reasons previously outlined. The difference in agreement in the medium energy region appears primarily to be due to the inclusion of the additional (σ) process.

ACKNOWLEDGMENTS

The authors would like to acknowledge the assistance of Dr. D. G. Coyne, who was doing an experiment using the same apparatus. Dr. E. D. Alyea, Jr., contributed much in the early days of the experiment. Special mention is due Herb Juds and Harry Coffey for help with the bubble chamber and the scanning equipment. The list of scanning personnel is too long to enumerate, but their help is gratefully acknowledged, as is that of the staff and personnel of the synchrotron laboratory.